International Journal for Modern Trends in Science and Technology, 9(03): 211-217, 2023

ISSN: 2455-3778 online
DOI: https://doi.org/10.46501/IJMTST0903032
Available online at: http://www.ijmtst.com/vol9issue03.html

Solar-Powered Off-Board Domestic Charging Station Design for Electric Vehicles

Rajendra Kodamanchili, P.Ramya Sai, B. Ramya, K. Srinivasa Rao, P.Venkateswara Rao

Department of Electrical Engineering, Ramachandra College of Engineering, Andhra Pradesh, India

To Cite this Article
Rajendra Kodamanchili, P.Ramya Sai, B. Ramya, K. Srinivasa Rao and P.Venkateswara Rao. Solar-Powered Off-Board Domestic Charging Station Design for Electric Vehicles. International Journal for Modern Trends in Science and Technology 2022, 9(03), pp. 211-217. https://doi.org/10.46501/IJMTST0903032

Article Info
Received: 28 February 2023; Accepted: 18 March 2023; Published: 19 March 2023

ABSTRACT

In this work, we show how to construct and simulate a solar-powered off-board EV charging station for home use by using a variety of converter topologies. Typically, a DC off-board charger will include an input source of electricity and a DC-DC convert for voltage corrections in order to provide an output voltage that is in line with the battery's nominal voltage. A power point maximum tracker (MPPT) is necessary to capture the peak power output of a photovoltaic systems (PV) array and send it to the converter's input. More effective converter topologies are constantly being developed and tested. This study chooses three of the most common DC-DC converter topologies: the full bridge DC-DC converter with a high frequency transformer, the double end primary inductance converter (SEPIC), and the DC-DC boost converter. The simulation findings for these topologies in the Simulink/Matlab environment are discussed in detail.

Keywords- Solar PV, EV charging station, DC-DC boost converter, SEPIC converter, full bridge DC-DC converter.

1. INTRODUCTION

Yet, electric cars are predicted to outperform their gasoline-powered counterparts in regards to power distribution without significantly reducing their driving range. The focus of the globe will soon be on electric automobiles, and by 2030, it is predicted that the vast majority of nations would sell nothing but electric vehicles. It was also announced that by 2030, India will actively encourage the use of electric cars. As a consequence, there has to be a nationwide network of business and residential charging stations set up [1]. A large number of charging stations will need to be self-sufficient, relying on local renewable energy sources to serve outlying and island communities [2], [3]. Solar energy is only accessible during the day, and the amount of sunlight that reaches a given location at a given time varies depending on a number of variables. Power trackers that are both efficient and easy to use are essential for getting the most out of a solar power system [4, 7]. The ability to store energy for use during times of both high and low demand is a crucial feature of modern energy infrastructure. For maximum performance and to prevent damage from overcharging, experts are working to perfect battery management systems [8]. There has been a lot of talk about using AI and machine learning to create a new kind of charger [9]. The two main components of a DC charging station are the converter and the control circuit. Design and efficiency considerations vary depending on the converter topology utilised in a

charger. There are fewer parts needed for the DC-DC buck converter than there are for the other two schemes. In comparison to the SEPIC architecture, the converter performs quite well in terms of efficiency. Nevertheless, the output voltage of the PV array must be maintained at a level lower than battery terminal voltage [10–13], hence there is a fundamental limitation to the MPPT performed area in this system. As the SEPIC architecture requires both current and voltage sensors for MPPT functioning, the quantity of parts utilised is greater than in the other two topologies. As a result, the charging mechanism becomes more expensive and operates more slowly. Having both sensors active also raises algorithmic complexity. The voltage sensor has one important drawback: it shortens the time the battery spends being charged at voltage level, which causes corrosion and shortens the battery's lifespan. [14]-[15]. Although the DC-DC converter is so much more efficient, the Multilevel inverter is not. The SEPIC architecture is conceptually similar to that of the Cuk and Zeta converters. Cuk converters provide an infinite zone for MPPT implementation and a diverse selection of output voltages, but they are limited by a negative DC-DC converter output supply. A zeta converter lowers the effectiveness of a solar panel. The complete bridge conversion with high-frequency transformers (HFT) is more challenging to design from a cost standpoint. For the operational amplifier DC-DC converter, a switched-mode energy supply was the starting point for the design (SMPS). For galvanic separation between input and output, HFT is used. Low harmonics in the input supply and a high current factor are the outcomes. [16]-[17]. In this study, we will examine the fundamentals of electric car chargers in an effort to better design and model these fundamental types of converters. This practise contributes to the creation of a practical and economical answer for off-board charger units in constrained business and residential settings. The method may serve as a starting point for the development of cutting-edge smart charging methods. The DC-DC boost converter, the SEPIC, and the complete bridge converter employing an HFT are the three converter technologies investigated in depth and evaluated in terms of component need and efficiency in order to design the EV charger. Every one of the topologies is provided together with the circuitry design and execution. Last but not least, the Simulink/Matlab environment is used to show off the simulation findings.

II.CHOSEN TOPOLOGIES FOR CHARGERS

In fig. 1, we see a straightforward DC-DC charger powered by solar photovoltaics. A solar photovoltaic module serves as the primary source, while a converter topology and an end user's devices round out the rest (battery pack).

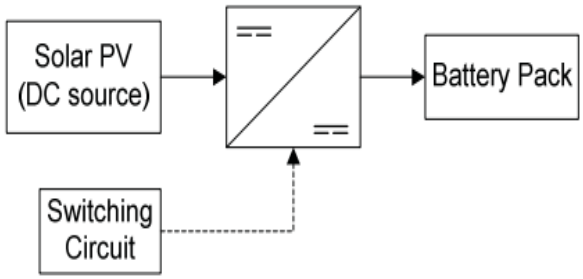

Fig. 1. Schematic diagram of a solar PV based DC to DC charger.

A.Battery charger that uses a DC-DC boost converter fueled by solar energy

A boost converter is seen in Fig. 2 being used to charge an electric vehicle (EV). This is accomplished by using a direct current (DC) to direct current (DC) power converter to raised the voltage to a level required by the battery bank.

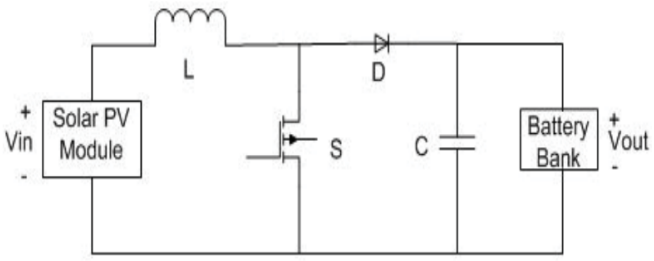

Fig. 2.DC-DC charger using boost converter

Boost converters may function in any of two ways. At the first setting, the switch acts as a short circuit, allowing electricity to flow with almost little resistance. The valve and the DC power supply form a loop through which current flows. This causes the ON-state inductor current to steadily increase up to a maximum value, following a positive slope. A negative slope returns the current to its starting value. Thus, the inductor current doesn't fluctuate at all during the course of a single cycle. The following setting corresponds to an open switch and forward bias in the diode, and is achieved by toggling the switch.

$$D = 1 - V_{in}/V_{out} \quad (1)$$

The polarity of the inductor has been flipped. The load is where the inductor's stored energy is finally used. The direction of the current is the same.

If Vin is the voltage at the input, then Vout must be the voltage at the output.

$$L = \frac{V_{in}*(V_{out}-V_{in})}{\Delta I_L * f_S * V_{out}} \quad (2)$$

Using this formula, we can get the inductor's value (L).

Ripple current in the inductor is approximated as, and the duty cycle of the converter is fs.
The capacitance (C) may be determined using the formula:

$$C = \frac{I_{out}*D}{f_S * V_{out}} \quad (3)$$

Where,
I_{out} is the output current.

B.Solar powered SEPIC converter for the battery charger

The SEPIC architecture for charging electric vehicles is seen in Fig. 3. In this case, the output voltage from the converter is either lower than, higher than, or the same as the input voltage. The duty ratio of the remote control determines the output

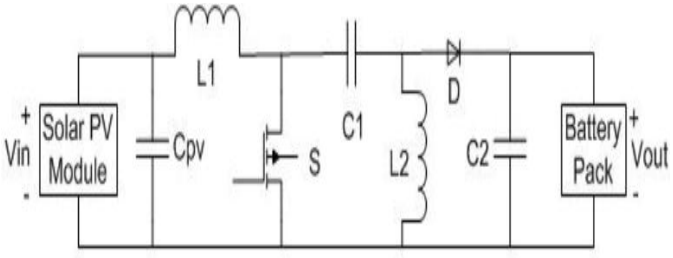

Figure 3.SEPIC topology DC-DC charger

With the SEPIC, you may choose between two different modes. The IGBT is active whenever the pulse is strong. Input voltage.The voltage from Vin is used to charge the capacitor C1, which in turn charges inductor L1. The voltage stored across capacitor C2 is the output when the diode is turned off. So when pulse is weak, the IGBT is turned off, and the diode allows current to flow to the load while charging the capacitors [8]. More power is generated at higher duty cycles because charging an inductor for longer results in a higher voltage.
Here's an equation for determining the duty ratio (D) given the input and target values for y:

$$D = \frac{V_{out}}{V_{in}+V_{out}} \quad (4)$$

Assume a circuit with a fixed input voltage V in and a variable output voltage V out.

Shorter charging and discharging times are available for PV output capacitors with lower values (%&'). As a

$$C_{PV} = \frac{\Delta I_{PV}}{8*\Delta V_{PV}+f_S} \quad (5)$$

result, it's crucial to have the right dimensions for this capacitor. While calculating Cpv, we use the formula:
To set the converter's switching frequency, type.

The following equations may be used to determine the values of inductors L1 and L2:

$$L_1 = \frac{D*V_{PV}}{f_S*\Delta I_{L1}} \quad (6)$$

$$L_2 = \frac{(1-D)*V_{batt}}{f_S*\Delta I_{L2}} \quad (7)$$

The following equations may be used to determine the values of capacitors C1 and C2:

$$C_1 = \frac{D*I_{batt}}{f_S*\Delta V_{Cm}} \quad (8)$$

$$C_2 = \frac{D}{R\left(\frac{\Delta V_{batt}}{V_{batt}}\right)f_S} \quad (9)$$

C.High-frequency transformer battery charger using solar-powered full-bridge converter

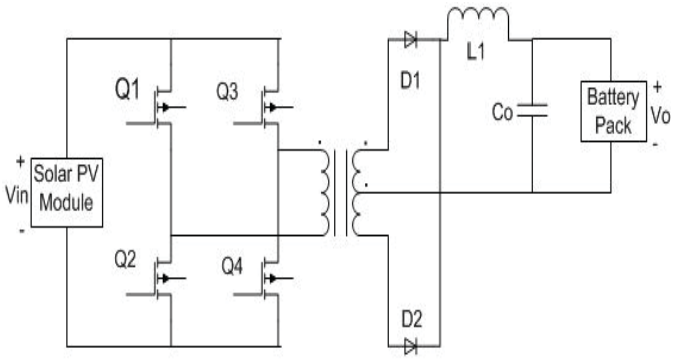

Figure 4: DC-DC charger with a complete bridge converter architecture.

Switches are alternately ON in each half cycle of the pulse width modulation period. The converter has two time bases for its operations. Interval 1 in the initial half cycle has Q1 and Q4 switched on. The load receives power through the HFT and the rectifier. In period 2, the load current passes through the diodes since all four valves are off. Controls Q3 & Q2 are ON in interval 1 of the next half cycle, and all switches are OFF in interval 2.

These are some formulae that may be used to determine the values of the circuit and the capacitor:

$$L_1 = \frac{(0.5-D)V_o * T_s}{\Delta I_L} \qquad (10)$$

$$C_O = \frac{D * I_o * T_s}{\Delta V_O} \qquad (11)$$

The following equations are used to determine the nominal input as well as output voltage (VinD,VoutD) and the theoretical input and exit current (IinD,IoutD) while designing an HFT:

$$V_{in-D} = V_{in} * D_{max} \qquad (12)$$

$$V_{out-D} = V_o + 1.6 \qquad (13)$$

$$I_{out-D} = I_o * D_{max} \qquad (14)$$

$$I_{in-D} = I_{out-D}/n \qquad (15)$$

$$n = \frac{V_{in-D}}{V_{out-D}} \qquad (16)$$

3. SELECTION OF PHOTOVOLTAIC ARRAY AND MPPT ALGORITHM

SolarPhotovoltaicArray

In the Matlab/Simulink environment, the charger is simulated using the PV array block in theSimulink library. Each PVmodule has 60 solar cells, and 10 modules may be linked in series to provide a usable amount of energy. The module is provided with real-time data from the PVGIS-5 geo-temporal irradiation database, including irradiance and temperature measurements taken at a particular location (Latitude: 17.372, Longitude: 78.456). Intensity of radiation varies from zero to six hundred fifty watts per square metre.

MPPTAlgorithm

In order to create the maximum power point tracking (MPPT) mechanism, the perturbed observer method is implemented. Fig.7 is a flowchart depicting the reasoning used to determine the duty cycle of the converter based on the MPP value. Voltage is adjusted in this manner by measuring the resulting difference (V). When the voltage shifts, we can determine the power's differential shift, or dP. When there is no change in power, it means that maximum output has been attained. The power shift may not be zero in less-than-ideal circumstances. If 0V results in 0P, then the direction of the disturbance is saturnine; otherwise, it is antisaturnine.

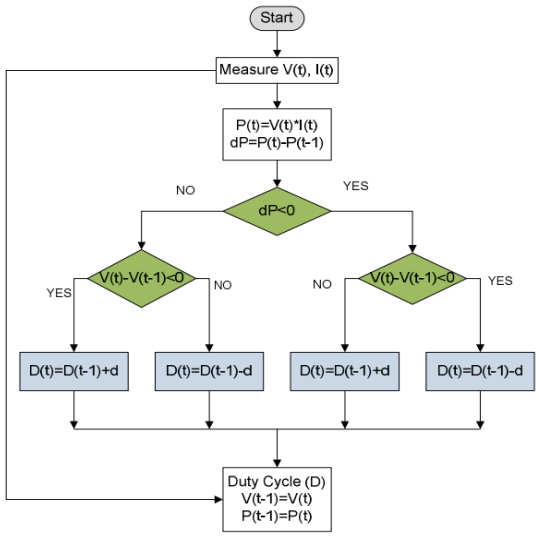

Fig. 5: Flowchart of the Actualized MPPT Method

The output is based on a comparison between the measured voltage V(t) and the calculated current I(t) from the preceding time step, t-1.

$\Delta V = V(t) - V(t-1)$ and

$\Delta P = P(t) - P(t-1)$.

The duty cycle delta (D(t)) is similarly approximated as D(t) = D(t -1) d, where d is the step size used in the MPPT approach for the created system.

4. SIMULATION AND RESULTS

In this part, we use MATLAB and Simulink to model and simulate our chosen topologies. The Embedded MATLAB

A. Simulation of a solar-powered DC-DC power converter rechargeable battery

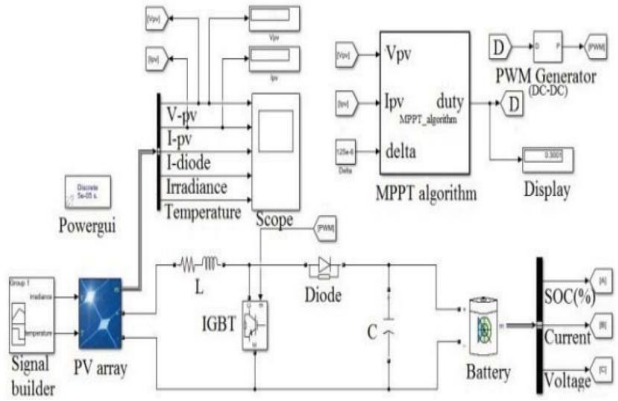

Fig. 6.Modeling a power converter DC-DC chargers in Simulink

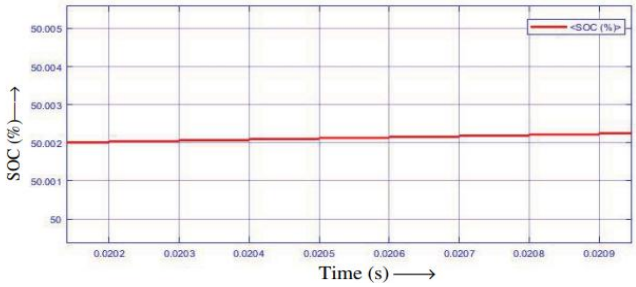

Fig. 7(a). The boost converter topology battery SOC vs. time graph

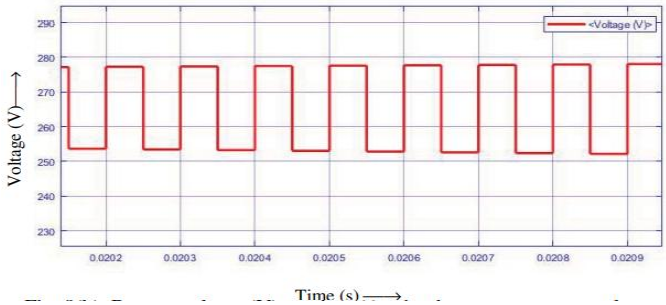

Fig. 7(b). Boost converter topology battery voltage vs. time graph

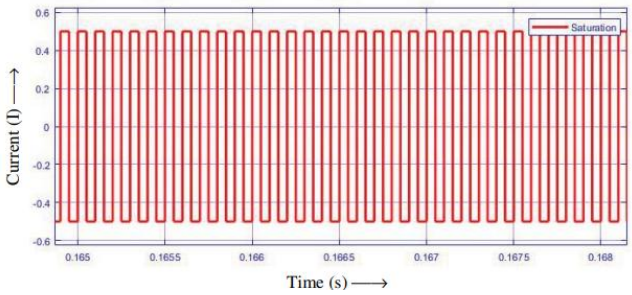

Fig. 7(c). the current drawn from a battery as a function of time (t) using a boost converter topology

B.Using the SEPIC architecture, a solar-powered battery charger is simulated.

Based on the charger's input and output characteristics, the SEPIC architecture is developed and the cost of the component is determined. Our calculations indicate that D = 0.6 is the appropriate duty cycle. The 0.69 mH & 1.67 mH inductors are removed. The converter uses 12 F and 0.3 F capacitors in its construction. The created Simulink model is executed by means of the fixed-step solver ode3. In order to display and analyse the output, the indicators of the solar PV array, converter, and battery characteristics are stored in the workspace window. Figure 10 depicts the model used in the simulation, and Figures 11(a)-11(c) illustrate the resulting performance (c).

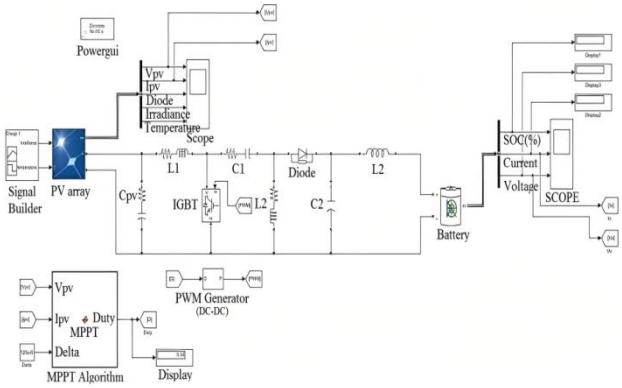

Fig.8:Simulink model of a DC-DC charger implemented in the SEPIC topology.

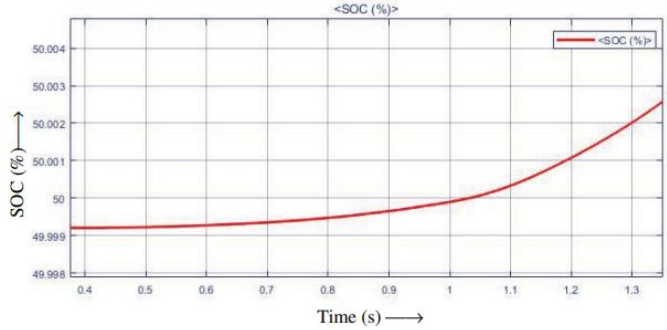

Fig. 8(a). Figure 8 shows a Simulink of a SEPIC topology DC-DC charger.

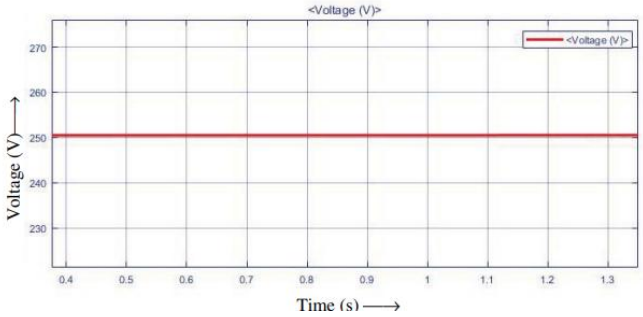

Fig. 8(b). SEPIC topology battery voltage vs. time graph

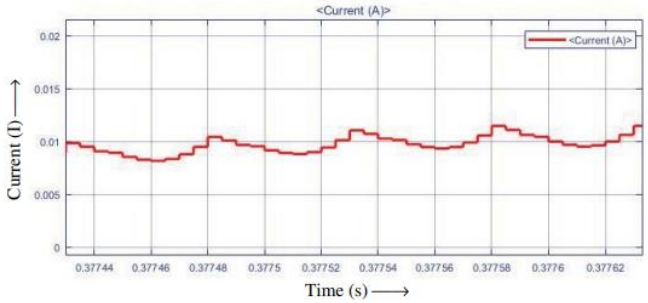

Fig. 8(c). SEPIC topology charge power (I) vs. runtime (t)

C.Modeling and simulation of a solar-powered full-bridge converter high-frequency transformer battery charger

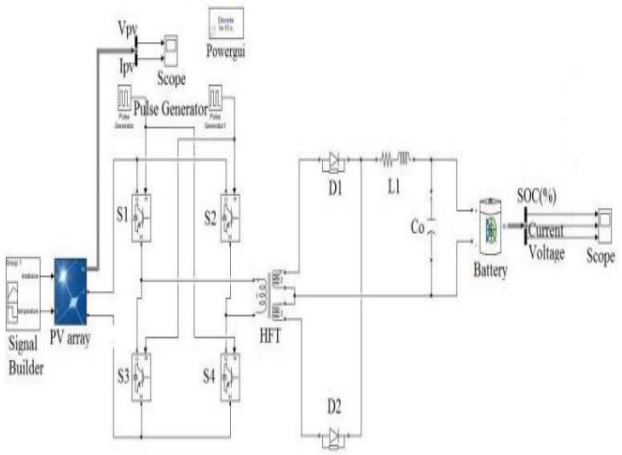

Fig. 9. Modeling a complete bridge converter HFT topology DC-DC charger in Simulink

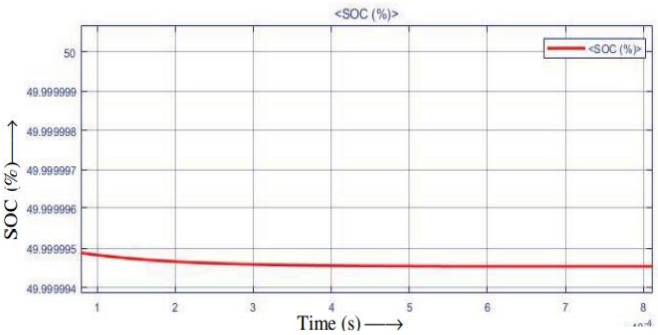

Fig. 9(a). Whole bridge converter topology battery level of charge (SOC) vs time (t)

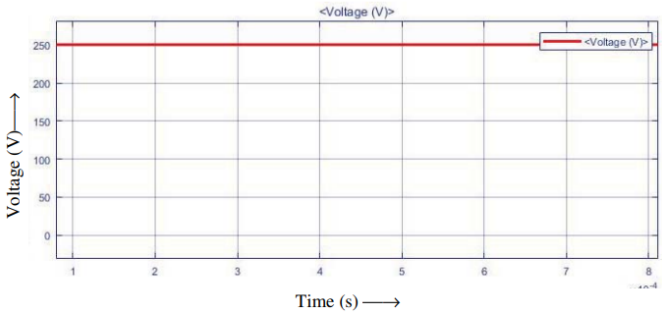

Fig. 9(b). Whole bridge converter topology battery voltage vs. time graph

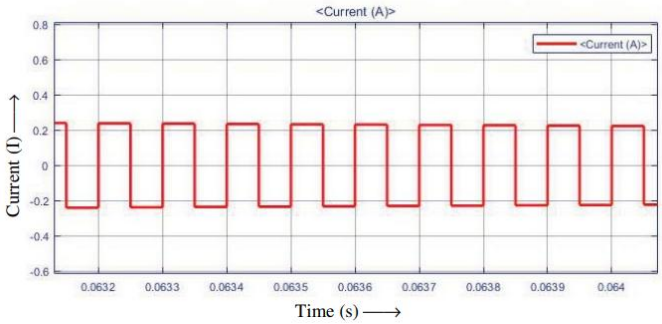

Fig. 9(c). Whole bridge converter topology battery power (I) vs. time (t)

The complete bridge converter has an average output voltage of 250 V. The duty cycle effectively follows the solar PV's maximum power output throughout a wide range of illumination conditions. Right now the battery is set to charge. By isolating the input and output of the power supply, the ultrasonic transformer may lower the amount of harmonic distortion. The adopted architecture has effectively optimised the battery by increasing the PV voltage, leading to excellent system performance. Table I provides a comparison of the various converters we considered.

TABLE I. COMPARISON BETWEEN THE TOPOLOGIES

Converters Parameters	Boost converter	SEPIC	Full bridge converter
No. of switches	1	1	4
High frequency transformer	0	0	1
Ripple content	10% of output voltage	30% of output voltage	30% of output voltage
Efficiency	83.2%	66.7%	98.6%

5. CONCLUSION

In this study, we offer a solar-powered battery charging system that is both efficient and dependable. To determine the most effective topology, we have tested

and evaluated their respective performance results. Using MPPT technology, maximum power is consistently extracted from solar PV at all light intensities. Those are the most parts needed for the complete bridge converter, following by the SEPIC design. In terms of parts, the boost converter is among the most minimalist. As compared to the other two topologies, the complete bridge converter stands out as the most efficient. From this, smart charging solutions based on emerging technologies like artificial intelligence and machine learning may be developed.

Conflict of interest statement

Authors declare that they do not have any conflict of interest.

REFERENCES

[1] F. G. Martínez, G. L. Magaldi, and F. M. Serra, "Solar Charging Station for Small Electric Vehicles," presented at the Argentine Conference on Automatic Control (AADECA), Buenos Aires, 2018, pp. 1-6.

[2] Pavan M. N., Vijayendra V. K., and Shashikala M. S., "SelfSustainable off grid Electric Vehicle (EV) Charging Station with Integration of Renewable Sources," International Journal of Engineering and Advanced Technology (IJEAT), ISSN: 2249 – 8958, vol. 9, no. 3, Feb. 2020.

[3] Otward M. Mueller and Eduard K. Mueller, "Off-Grid, Low-Cost, Electrical Sun-Car System for Developing Countries," presented at the IEEE Global Humanitarian Technology Conference, San Jose, CA, USA, Oct.10-13, 2014.

[4] Tekeshwar Prasad Sahu and T. V. Dixit, "Modelling and analysis of Perturb & Observe and Incremental Conductance MPPT algorithm for PV array using 0uk converter," IEEE Students' Conference on Electrical, Electronics and Computer Science, Bhopal, India, April 24, 2014.

[5] Chihchiang Hua and Chihming Shen, "Study of maximum power tracking techniques and control of DC/DC converters for photovoltaic power system," 29th annual IEEE Power Electronics Specialists Conference, vol. 1, May 1998.

[6] M. Killi and S. Samanta, "Voltage-Sensor-Based MPPT for StandAlone PV Systems Through Voltage Reference Control," IEEE Journal of Emerging and Selected Topics in Power Electronics, vol. 7, no. 2, pp. 1399-1407, June 2019.

[7] Y. Hu and J. Zhang, "Efficiency Improvement of Non uniformly Aged PV Arrays," IEEE Trans. on Power Electronics, vol. 32, no. 2, pp. 1124-1137, Feb. 2017.

[8] Yu Miao, Patrick Hynan, Annette von Jouanne, and Alexandre Yokochi, "Current Li-Ion Battery Technologies in Electric Vehicles and Opportunities for Advancements," Energies 2019, 12, 1074; doi:10.3390/en12061074

[9] N. Liu, Q. Chen, X. Lu, J. Liu, and J. Zhang, "A Charging Strategy for PV-Based Battery Switch Stations Considering Service Availability and Self-Consumption of PV Energy," IEEE Transactions on Industrial Electronics, vol. 62, no. 8, pp. 4878-4889, Aug. 2015.

[10] V. V. Joshi, N. Mishra, and D. Malviya, "Solar Energy Integration with New Boost Converter for Electric Vehicle Application," in Proc. 8th IEEE India International Conference on Power Electronics (IICPE), Jaipur, India, 2018, pp. 1-6.

[11] S. A. Arefifar, F. Paz, and M. Ordonez, "Improving Solar Power PV Plants Using Multivariate Design Optimization," IEEE Journal of Emerging and Selected Topics in Power Electronics, vol. 5, no. 2, pp. 638-650, June 2017.

[12] A. M. Khatib, M. I. Marei, and H. M. Elhelw, "An Electric Vehicle Battery Charger Based on Zeta Converter Fed from a PV Array," in Proc. IEEE International Conference on Environment and Electrical Engineering and 2018 IEEE Industrial and Commercial Power Systems Europe (EEEIC / I&CPS Europe), Palermo, 2018, pp. 1-5.